Nanofiber-Reinforced Thermoplastic Composites. I. Thermoanalytical and Mechanical Analyses

K. LOZANO,[1] E. V. BARRERA[2]

[1] Department of Engineering, University of Texas Pan American, Edinburg, Texas 78539

[2] Department of Mechanical Engineering and Materials Science, Rice University, Houston, Texas 77005

Received 9 September 1999; accepted 30 April 2000

ABSTRACT: This article is a portion of a comprehensive study on carbon nanofiber–reinforced thermoplastic composites. The thermal behavior and dynamic and tensile mechanical properties of polypropylene–carbon nanofibers composites are discussed. Carbon nanofibers are those produced by the vapor-grown carbon method and have an average diameter of 100 nm. These hollow-core nanofibers are an ideal precursor system to working with multiwall and single-wall nanotubes for composite development. Composites were prepared by conventional Banbury-type plastic-processing methods ideal for low-cost composite development. Nanofiber agglomerates were eliminated because of shear working conditions, resulting in isotropic compression-molded composites. Incorporation of carbon nanofibers raised the working temperature range of the thermoplastic by 100°C. The nanofiber additions led to an increase in the rate of polymer crystallization with no change in the nucleation mechanism, as analyzed by the Avrami method. Although the tensile strength of the composite was unaltered with increasing nanofiber composition, the dynamic modulus increased by 350%. The thermal behavior of the composites was not significantly altered by the functionalization of the nanofibers since chemical alteration is associated with the defect structure of the chemical vapor deposition (CVD) layer on the nanofibers. Composite strength was limited by the enhanced crystallization of the polymer brought on by nanofiber interaction as additional nucleation sites. © 2000 John Wiley & Sons, Inc. J Appl Polym Sci 79: 125–133, 2001

Key words: nanofibers; thermoplastic composites; thermal analysis; vapor-grown carbon fibers; single-wall nanotubes

INTRODUCTION

Carbon nanofibers have been recognized as interesting materials with applications that seem promising in nanoscale technology. Nanofibers, which include multiwall, single-wall, and carbon fibrils, have average diameters of less than 100 nm. Their electrical, thermal, and mechanical properties make them promising as composite fillers and reinforcements. Although some investigators have noticed the practical use of nanofibers for conducting polymers, thermal systems, and structural materials,[1–3] and some others have shown polymer composites with dispersed nanofibers,[4,5] little has been done to understand the nature of the processing and the thermal behavior of the polymer–nanofiber mixtures. In this study

Correspondence to: K. Lozano.

Contract grant sponsor: National Science Foundation; contract grant number: DMR-9357505.

Contract grant sponsor: Texas Higher Education Coordinating Board; contract grant number: 003604-056

Contract grant sponsor: National Aeronautics & Space Administration; contract grant number: NCC 9-77

Journal of Applied Polymer Science, Vol. 79, 125–133 (2001)

vapor-grown carbon fibers (VGCFs) were mixed into a polypropylene (PP) matrix to form nanofiber composites. The hollow-core VGCFs are an ideal precursor to working with multiwall and single-wall nanotubes when more conventional polymer processing is to be used. Current limitations on using Banbury-type mixing, including extrusion for nanotube composite processing, are related to the low availability of nanotube materials. For this study composites were prepared using conventional polymer-processing technologies, which require material that's an order of magnitude more than what's needed for minor bench-top mixing. A comprehensive study was conducted, starting with nanofiber purification and functionalization, and then composite isotropic mixing and thermophysical characterization including microscopy and thermal, electrical, rheological, dynamic, and mechanical analyses of the composite. Past studies have sought specific applications of the composites as electrostatic discharge materials and structural composites. A goal of this work was to produce uniformly dispersed nanofibers in a polymer matrix with the absence of agglomerates and porosity. This article is a portion of a comprehensive study and focuses on thermal behavior and dynamic and tensile mechanical properties of the nanofiber PP composites. The rheology and conducting polymer applications of these composites will be discussed in a subsequent article.

The thermoplastic matrix PP was selected because thermoplastics are now receiving increased interest due to their manufacturing versatility, high strength, and stiffness.[6] The recyclability of thermoplastics gives it an advantage because subsequent processing is to be used in this study (pelletizing, extrusion, and/or rheological evaluation). PP was chosen since it has been well studied and could be obtained as a homopolymer.

The influence of various fillers and reinforcements on the nucleation, crystallization, mobility of the macromolecules, molecular alignment, crystal structure are well understood for micro to macro fillers including carbon fibers and carbon black.[7-18]Little has been done to comprehend whether the nanoscale reinforcements produce alternate behaviors in the polymer nucleation and crystallization processes especially since the nanofibers have two to four orders of magnitude more surface area and that same degree of lesser space between the fibers than micron size carbon fiber composites. The present study focuses on identifying the effects of the nanofibers on the thermophysical properties of the composites. Polymer crystallinity, thermal degradation, and dynamic and tensile mechanical analyses were studied. For a given set of processing parameters and a broad composition range of nanofibers an understanding of the contributions of these reinforcements in a polymer thermoplastic have been resolved.

Background

Nanofibers notably have macromolecules about the same size as polymers. Therefore, nanofibers, whether in a thermoplastics or thermosetting epoxy are likely to alter the physicochemical properties of the composites in a more pronounced way than macro-size fibers. It becomes increasingly important to understand the thermal behavior of the polymer as the nanofiber composites are formed. This will be well understood as polymer selection and composite design are better tailored for the inclusion of nanofibers. Current nanofiber composite studies select polymeric systems based solely on ease of processing, along with some interest in achieving bonding. It seems evident that polymer design will be necessary before significant enhancement in mechanical properties of nanofiber composites can be achieved, although electrical and thermal enhancements may be achieved in the near term.

The processing of any polymer or composite can cause matrix degradation leading to macromolecular chain breakage and resulting in low-molecular mass products.[7,19,20] With PP, degradation can occur by cleavage of the carbon—carbon bonds at the bond adjacent to the methyl groups because these are the weakest bonds. Polymer additions can enhance physical properties by acting as restriction sites, reducing the tension induced in the carbon—carbon bonds by thermal excitation and consequently increasing the thermal stability of the polymer. They may also act as antioxidants, reacting with incoming oxygen and therefore driving the polymer to a higher temperature before degradation.[7,20] The thermal working range of the polymer can be increased while the other physical properties of the composite are also enhanced (i.e., electrical and thermal). However, other aspects of the polymer may be altered to the point that, in the case of mechanical properties, an alteration of the matrix crystalline structure may limit the influence of the reinforcing nanofibers. In the case of crystalline or semicrystalline polymers, crystallization can be influ-

enced by fillers and additives to reduce its effectiveness as a composite matrix. Work conducted by Marosi et al.[7] with $CaCO_3$ as filler for PP showed an increase in the degree of crystallinity. They concluded that the increased mobility of the macromolecules leading to further crystallization was caused by the modification of the interfacial layer around the $CaCO_3$. Amash and Zugenmaier studied changes in the crystallization of PP reinforced with glass fibers and polyester fibers. In this situation both these fibers caused an increase in the rate of crystallization without modifying the degree of crystallinity.[12] Ahmad et al. studied the crystallinity of PP–rice husk ash composites, observing a concentration-dependent change in crystallinity and the rate of crystallization.[11] Petrovic et al. reported a decrease in crystallinity of PP filled with carbon black,[21] yet carbon black tends to increase the crystallinity of elastomers, resulting in "bound rubber."[22,23] Although the changes that occur are discussed in terms of rate and degree of crystallization, the true influence may be in the alteration of nucleation, which drives the crystallization process. In short, dispersed nanofibers may well alter polymer crystallinity to grossly affect polymer matrix properties.

Dynamic mechanical analysis can provide an understanding of the viscoelastic behavior of the nanofibers–PP composites. Viscoelastic measurements are sensitive indicators of internal structure and as such can be used to develop structure/property relationships of polymer systems.[24–31] The dynamic storage modulus and the loss factor are the two main variables that determined the mechanical effect of the nanofibers on the PP. In the case of the tensile measurements, it is expected that the structural reinforcement will be hampered by the strong interactions between the fiber and semicrystalline matrix because of changes in crystallinity. Given the size of the nanofibers, it is possible that the amorphous phase will be immobilized by the nanofibers, resulting in a stiffer, less flow-resistant material.

EXPERIMENTAL

Materials

For this research, carbon nanofibers (Pyrograf-IIITM) were provided by Applied Sciences (Cedarville, OH). Pyrograf are carbon nanofibers produced by the vapor-grown carbon fiber production method, which is a catalytic process of hydrocarbons in the vapor state (in some cases these nanofibers are called fibrils). VGCFs have circular cross sections (with diameters varying from 20 to 200 nm) and central hollow cores commonly called filaments. The nanofiber graphitic networks are arranged in concentric cylinders of annular carbon layers that have an intrinsic structure formed by a tree-ring configuration.[32–35] This configuration is what gives the fibers their physical properties of high tensile strength, modulus, and electrical and thermal conductivity. Its thermal conductivity (1950 W/m − K) is the highest among all other commercial carbon fibers and has one of the highest values found in nature except for diamonds.[33] Kilogram quantities are available from the manufacturers, enabling composite development at a higher scale than that seen in current multiwall and single-wall composite research.[25,36,37] Several sources of these nanofiber systems are now available,[38,39] and these nanofibers may well provide demonstrated composite systems in the near term.

Table I Physical Properties of Polyproplyene in As-Received Condition

Type	Homopolymer
Density: gm/cc	0.909
Tensile Strength @ yield (MPa)	36
Flex Modulus: (Gpa)	1.24
Deflection temperature (°F @ 0.4 Mpa)	101
Melt Flow Rate (g/10 min)	2

Polypropylene is a very well-known thermoplastic and is commercially available in different grades with different types of additives. It is a nonpolar semicrystalline polymer with low surface tension. PP HLM-020 from Phillips Sumika, Houston, TX was selected as the composite matrix in pellet form. It was selected as a natural homopolymer where PP–nanofiber interactions could be isolated. Table I lists the various properties of this thermoplastic system.[40]

Composite Manufacturing of Nanofiber-Reinforced PP

VGCFs were received as as-received (RAW) and as pelletized (PELL) material. Microscopic observation showed that a significant degree of purification was necessary to isolate nanofiber–polymer interactions in the produced composites. Purification and chemical functionalization processes

were developed to produce high-purity open network nanofibers. Objectives of the purification (PU) and functionalization (FUNC) were to remove non-nanofiber material while opening up the nanofiber network for easy deagglomeration of the nanofibers and infiltration and shear processing of the polymer. The final form of the nanofibers was a loosely bound agglomerated powder of high-purity nanofibers that did not undergo any decrease in their lengths. This configuration provided ease of handling with less opportunity for airborne material.

Banbury-type mixing using a Haake polylab with a 30-g mixing bowl was used to mix the nanofibers both treated and untreated (RAW, PELL, PU, and FUNC) with the PP. Given the size and tendency of agglomeration of the nanofibers, the Banbury-type mixer provided a uniform distribution of the fibers by exposing the agglomerates to hydrodynamic stresses, thus forcing the agglomerates to break down and evenly disperse with no porosity. Nanofiber dispersion in the absence of porosity was a key aspect in the sample preparation because the physical properties of the finished composite are strongly governed by the dispersion of the fibers in the matrix. Although a nanofiber network, much like that for carbon black materials, would lead to a low-concentration electrostatic discharge material, interests also lie in producing homogeneously dispersed nanofibers by which optically transparent polymer films can be produced. Compositions ranging up to 60 wt % VGCFs were produced with samples weighing 18–22 g.

The rheological study showed that the best processing conditions were: mixing temperature, 165°C; rotational speed, 65 rpm (increasing up to 90 rpm for the last minute); and residence time, 12–15 min, depending on the chosen fiber concentration. A number of methods for mixing the PP pellets and nanofibers were determined based on studies using PP, PE, ASA, PET, acetal, ABS, and PEEK. After the mixing stage, the composites were hot-pressed (with 6–11 metric tons at 150°C–170°C) into thin sheets. The samples were then cut or pelletized according to the required specifications for TGA, DSC, DMA and tensile analysis.

Analysis

A DuPont thermogravimetric analyzer (TGA) requiring samples weighing between 10 and 20 mg was used for thermal analysis. The samples were scanned at temperatures ranging from 25°C to 900°C in air, at a heating rate of 5°C/min^{-1} (typical degradation occurs around 400°C). Values for moisture pickup, onset, and final degradation temperature of the composites were determined. Differential scanning calorimetry (DSC) analysis, using a TA Instruments DSC 2920 Modulated DSC with a nitrogen atmosphere and a sample size of 10$\pm$ 2 mg was used. Hermetically sealed sample containers were used in these experiments to avoid oxidation. In the anisothermal experiments the samples were heated at a rate of 10°C/min to 210°C and then cooled down at a rate of 10°C/min to 90°C. Samples were then heated at 10°C/min up to 200°C. In the case of the isothermal experiments the samples were also heated to 210°C and kept at this temperature for 7 min to diminish the influence of the previous thermal and mechanical history. The samples were rapidly cooled down and held at different crystallization temperatures to record the crystallization time. This temperature was held for about 20 min and then raised 10°C/min up to 190°C to analyze the melt behavior after isothermal crystallization. Dynamic oscillation measurements were performed with a DuPont 983 dynamic mechanical analyzer. Samples (10 mm $\times$ 6 mm) with different thicknesses (0.4–0.8 mm), depending on the VGCF concentration, were analyzed. Elastic modulus and mechanical damping of the composite were measured under a fixed-frequency mode. The measurements were performed from temperatures ranging from room temperature to 170°C, with a temperature increase of 10°C/min. Dumbbell-shaped samples for tensile testing were prepared using a pressure die. Tests were carried out in a Chattillon mechanical testing instrument at a strain rate of 0.0254 m/min (1 in/min) at room temperature. Experiments were conducted based on the ASTM D-638 standard.

RESULTS AND DISCUSSION

Thermal Stability of the Polymer Matrix

Nanofibers in the as-received (RAW) and pelletized (PELL) form were used and purified (PU) and functionalized (FUNC). Samples with compositions of 2, 5, 9, and 30 wt % were studied for thermal stability. with the 5 wt % compared as as-received, purified, pelletized, and functionalized material. Pelletized VGCFs have a latex sizing applied by Applied Sciences. Thermogravi-

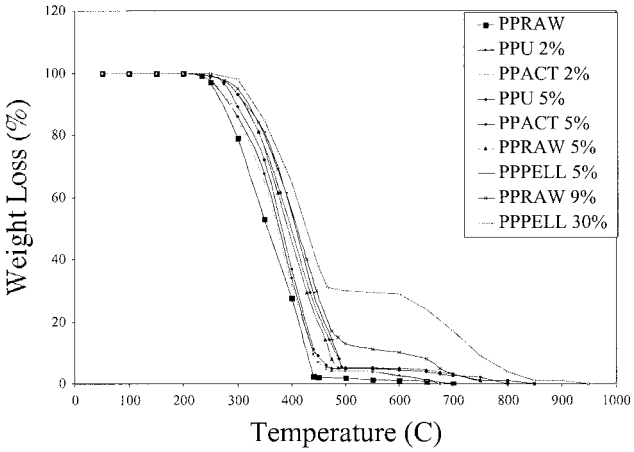

Figure 1 Thermogravimetric curves of the polypropylene homopolymer and the polymer composite samples with different fiber treatments.

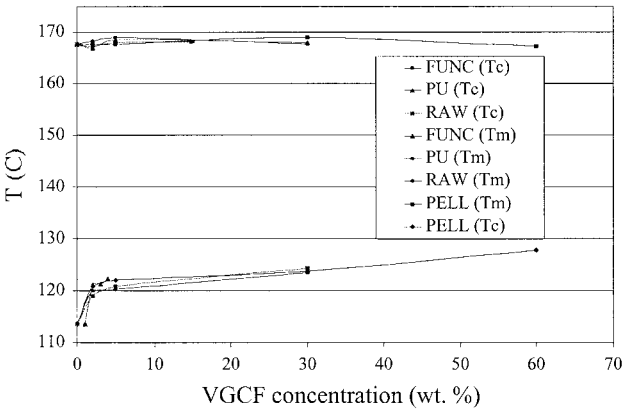

Figure 2 Effect of nanofiber concentration on the peak of crystallization (T_c) and melting (T_m) temperatures for nanofiber–reinforced PP composites.

metric analysis of the polymer composites samples is shown in Figure 1. The absence of weight loss from moisture pickup suggests that humidity of varying degrees might not affect performance. An increase in the onset of the degradation temperature occurs with increasing nanofiber concentration. This increase is independent of fiber treatment for the conditions studied. The increase in final degradation temperature (~100°C) can be explained by restrictions on the mobility of the macromolecules imposed by the VGCFs.[11] Since these fibers are nanosize, they impose a vast number of restriction sites, causing a reduction in the tension induced by thermal excitation in the carbon–carbon bond. Consequently, the thermal stability of the polymer increases significantly. Initial weight loss occurs solely in the polymer, up to a temperature of 500°C. The VGCFs are not affected until a temperature of 650°C is reached. The amount of VGCFs after complete polymer degradation corresponds to the initial VGCF concentration in the sample preparation process (see plateaus in the respective curves).

Matrix Crystallization

Crystallization and melting patterns (thermograms) were recorded during the cooling and heating processes for anisothermal measurement. From these thermograms, the thermal parameters of crystallization temperature (T_c), melting temperature (T_m), crystallization enthalpy (H_c), heat of fusion (H_f), and percentage of crystallinity (X_c) were obtained and are summarized in Table II. The degree of crystallinity was calculated from the crystallization enthalpy data where[12]

$$X_c = \frac{\Delta H_c}{\Delta H_c^o} \times 100 \quad (1)$$

The ΔH_f value used was 190 J/g, the theoretical value of enthalpy for a 100% crystalline isotactic polypropylene homopolymer.[12] Figure 2 shows an increase in the crystallization temperature from the addition of nanofibers, while the melt temperature was independent of VGCF content. Both temperatures were somewhat independent of the nanofiber preparation method. As the VGCF concentration was increased, the T_c continued to increase, suggesting that interactions between the fiber and the matrix are occurring. The increase in T_c is associated with an increased number of nuclei for crystallization, where a limiting number of crystallization nuclei seem to be reached at 5%, when a change in the nucleation rate is

Table II Crystallization Kinetics Parameters of VGCF-Reinforced Composites

Sample @ 130°C	T_c (°C)	T_m (°C)	ΔH_m (J/g)	X_c	N	K (min^{-1})
Pure PP	113.59	168.46	86.25	49.38	2.0366	0.0373
PP/5% VGCF	121.62	167.59	91.76	51.34	1.7559	0.3401
PP/60% VGCF	127.80	167.24	131.8	69.32	1.0000	0.8664

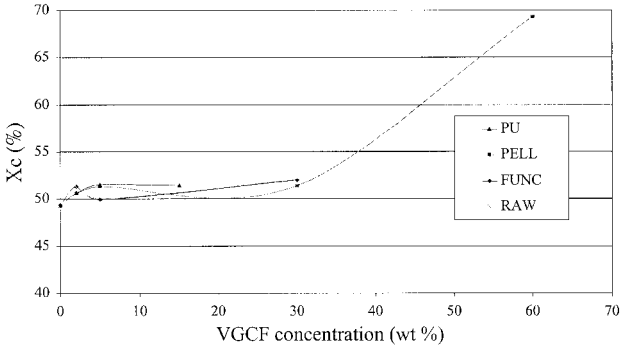

Figure 3 Percentage of crystallinity versus nanofiber concentration for the composites.

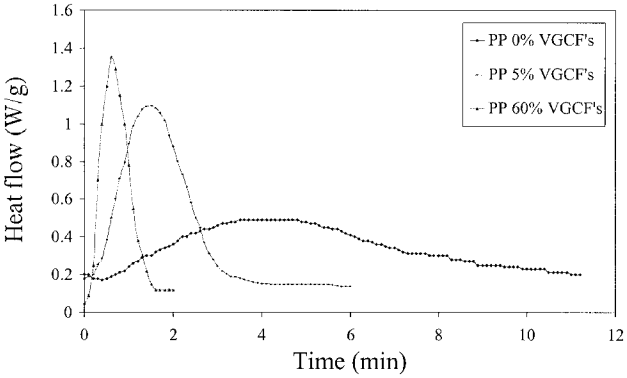

Figure 4 DSC isothermal crystallization curves for the nanofiber–reinforced PP composites at 130°C. Curves for pure, 5%, and 60% nanofiber concentrations are shown.

achieved. Therefore, the degree of supercooling ($T_m - T_c$) decreased with increasing VGCFs.[7,11,12,41,42]

The calculated crystallinity of the composites as a function of VGCF concentration is shown in Figure 3. At a concentration of 2% of functionalized and raw VGCFs, there is a noticeable increase, which can be explained as enhanced mobility of the PP macromolecular chains, leading to a better alignment of the crystal lattice. In the case of the purified and pelletized VGCF samples, this peak occurs at 5%. While the concentration of VGCFs increased, the fibers started to act as restriction sites for the PP segments, obstructing them from obtaining a highly ordered spherulite structure, and the crystallinity decreased. Above 10%, the crystallinity values start to increase again up to 3% over that of the pure homopolymer. In the case of the 60% pelletized VGCF sample, the percentage of crystallinity increased 20% over the homopolymer. In general, the degree of crystallinity and the rate of crystallization are affected by the presence of the fibers.

The overall crystallization rate can be determined by evaluating crystallinity at different times. The results of isothermal crystallization experiments for the samples with 0, 5, and 60 wt % of VGCF at 130°C are presented in Figure 4. From this thermogram, in which heat flow is plotted versus time, it can be observed that the time required to reach the exothermal DSC peak (T_c) decreases with increasing VGCF content. Therefore, PP with 60 wt % VGCFs crystallizes much faster than pure PP. The crystallization process can be evaluated according to the change in heat flow, while the rate of crystallinity can be studied using the Avrami equation[41–43]:

$$\alpha = 1 - \exp(-kt^n) \tag{2}$$

where α is the crystallinity at time t, k is the rate constant of crystallization, and n is the Avrami exponent. The value of the Avrami exponent depends on the mechanism of nucleation and the geometry of the crystal growth, while k is dependent on parameters of nucleation and growth rate. These kinetics parameters can be inferred from the Avrami plot in which $\ln^{-\ln(1-Xc)}$ is plotted against $\ln(t_i - t_o)$ (Fig.5). Where X_c is the fraction of crystallinity developed at time t_i obtained as the area under the crystallization curve. The rate constant of crystallization is given by the following formula[8]:

$$k = \ln 2/(\tau_{1/2})^n \tag{3}$$

in which $\tau_{1/2}$ is the crystallization half time, or the time at which 50% of the crystallization occurs.

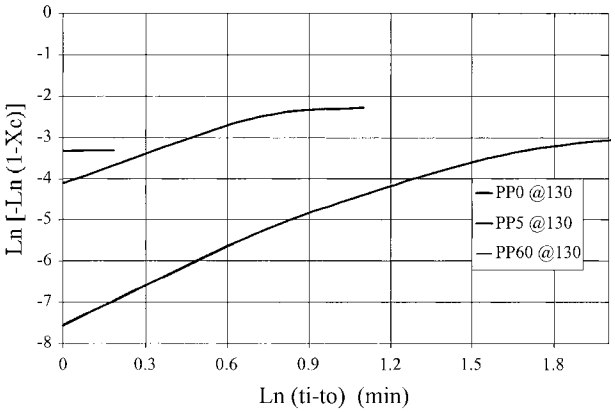

Figure 5 Avrami plot for nanofiber–reinforced PP composites at 130°C containing 0, 5, and 60% nanofiber concentrations.

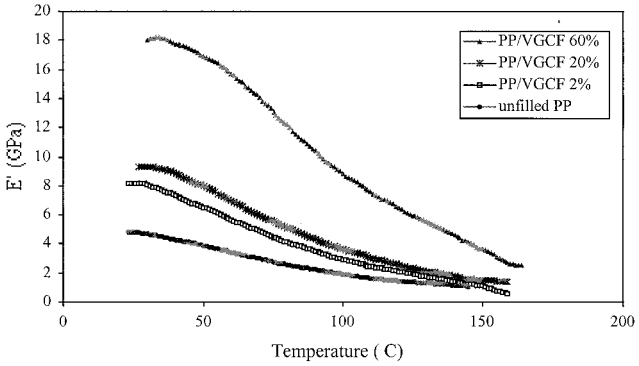

Figure 6 Dynamic mechanical curves showing the effect of nanofiber concentration on storage modulus for the nanofiber–reinforced PP composites.

The Avrami exponent, *n,* is given from the slope of the Avrami curves. The parameters of the kinetics, determined by the Avrami equation, are listed in Table II. According to Velasco et al., the ideal value for the Avrami exponent is 3, which implies a 3-D heterogeneous crystal growth.[41] Experimentally this value usually has nonintegral values that depend on the applied experimental method (DSC, dilatometry, and optical microscopy) and the development of lamellar and spherulitic entities (mixed nucleation modes) as well as in secondary crystallization factors. The values of the Avrami exponent of pure PP compares well to those reported in the literature.[19] Having analyzed the crystallization rate of PP and its composites under the same conditions, it can be concluded that the nanofibers induce the difference in the nuclei number. The increase in nucleation activity is resolved by the decrease in crystallization half time, $\tau_{1/2}$, and the increase in the rate constant of crystallization, k.

Dynamic Mechanical and Tensile Properties

Viscoelastic properties were mainly evaluated by the elastic modulus E′. E′ for different VGCF concentrations is shown as a function of temperature in Figure 6. Composite stiffness increased as the VGCF concentration increased. With increased VGCF content, the samples remained solid at higher temperatures, confirming the enhancement in thermal stability. Although E′ could only be measured for the unfilled PP up to a temperature of 145°C, the 60 wt % sample was measured up to a temperature of 165°C. It can also be observed from Figure 6 that the stiffness of the material increases significantly, even at a 2 wt % of nanofibers, where an increase in E′ of 100% at 30°C can be observed. In the case of the sample containing 60 wt %, an increase of 350% is observed.

The ultimate tensile strength and percent elongation results are shown in Table III. Tensile curves were similar to those for most thermoplastics, a restricted region of elastic response followed by regions of plasticity. As the nanofiber concentration was increased, the plastic range decreased considerably, which can be attributed in part to modifications in the crystalline fraction of the matrix. Restriction of the amorphous phase imposed by the isotropically deposited nanofibers plays a key role in this behavior. The restriction sites prevent the polymer from deforming, therefore causing a decrease in ductility and an increase in brittleness. The ultimate strength was not significantly altered by an increase in the fiber content. Although a direct enhancement of tensile strength has not been observed for these composites, possibly associated with a more brittle matrix condition, a detrimental strength condition also hasn't been seen, suggesting that nanofibers play a small role in strength enhancement. In addition, the unfilled PP exhibited a high value of elongation, 167%, decreasing to 13% at a 40% of VGCF content. This transition from ductile to brittle is associated with changes that occurred in the crystalline state of the matrix where the spherulite size was altered. Structural properties of this VGCF composite need further investigation, as can be observed from the high standard deviation values. Figure 7 shows two micrographs of a fractured composite where some degree of wetting is evident by the polymer extension around the nanofibers. Wetting was evaluated to be discontinuous and associated with the defect structure of the nanofibers since these are sites for functionalization. The 20% VGCF sample

Table III Tensile Properties for VGCF-Reinforced PP Composites According to VGCF Content

VGCF (wt %)	Tensile Yield Strength (MPa)	Ultimate Strain (%)	Standard Deviation
0	59	163	4.4523
5	69	67	1.5821
10	56	44	1.7214
20	50	69	3.4292
40	49	13	1.2220

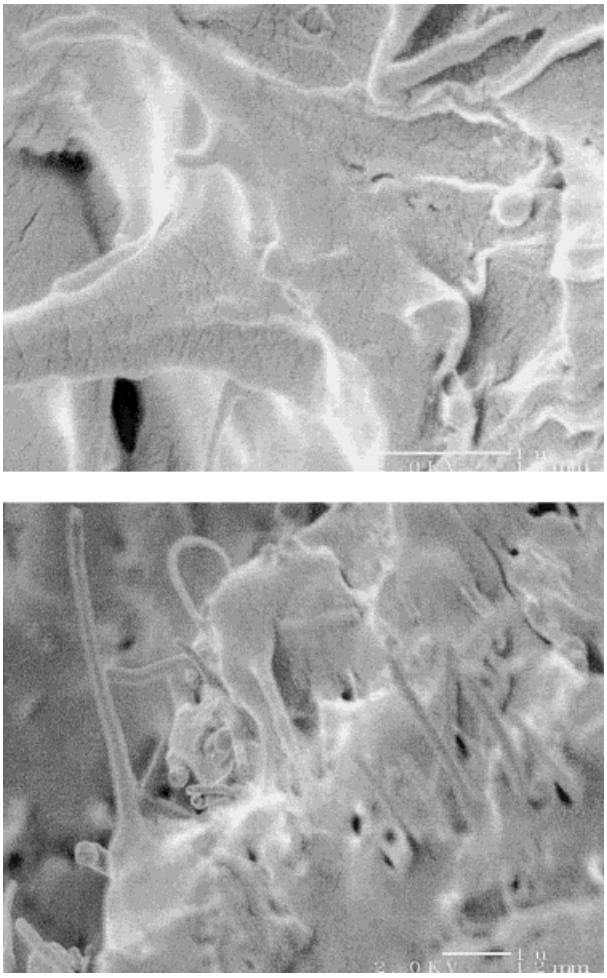

Figure 7 Scanning electron micrographs on wetting of the nanofibers by the PP matrix.

may show an entanglement nanofiber condition at about this composition, which could cause the sample to withstand higher strains.

CONCLUSIONS

The development of Nanofiber composites with a high degree of nanofiber dispersion has been achieved. The composites made with a nanofiber concentration of 2—60 wt % showed neither porosity nor nanofiber agglomerates. Thermal analysis of the composites showed the samples to have negligible moisture uptake and an enhancement in resistance to thermal degradation, as well as enhanced thermal stability, as seen by the higher temperature storage modulus measurements compared to those of the unfilled polypropylene samples. Polymer crystallization was influenced by the addition of the nanofibers. Nanofibers were evaluated for their actions both as antioxidants and as nucleating agents. Although a significant increase in the storage modulus occurred, no real change in the ultimate tensile strength of the composites was observed. The absence of strengthening of the composites was associated with the increased brittleness of the polymer matrix because of its inability to further crystallize on deformation, a property brought on by the molecular restrictions caused by the fiber dispersion.

Acknowledgments are due Dr. Jaime Bonilla-Rios for his helpful discussions.

REFERENCES

1. Ferguson, D. W.; Bryant, E. W. S.; Fowler, H. C. ANTEC 1998, 1219.
2. Schadler, L. S.; Giannaris, S. C.; Ajayan, P. M. Appl Phys Lett 1998,73, 26.
3. Friend, S. O.; Barber, J. J. U.S. Pat. 5,611,964 (1997).
4. Jin, L.; Bower, C.; Zhou, O. Appl Phys Lett 1998, 73, 9.
5. Chazeau, L.; Cavaillé, J. Y.; Canova, G.; Dendievel, R.; Bouthherin, B. J Appl Polym Sci 1999, 71.
6. K. Lozano; Ph.D. Thesis, Rice University, 1999.
7. Marosi, Gy.; Lgner, R.; Bertalan, Gy.; Anna, P.; Tohl, A. J Therm Anal 1996, 47.
8. Zhihui, Y.; Yajie, Z.; Jinghua, Y. Polymer-Plastics Technology and Engineering 1997, 36, 4.
9. Isasi, J. R.; Mandelkern, L.; Alamo, R. G. Polymer Preprints, Division of Polymer Chemistry, ACS Proceedings 1996, 37, 2.
10. Kenig, S.; Siberman, A.; Dolgopolsky, I. ANTEC 97, Vol. III, p. 2706.
11. Ahmad, M. Y.; Mustafah, J.; Mansor, M. S.; Mohd Ishak, Z. A.; Mohd Omar, A. K. Polym Int 1995, 38, 1.
12. Amash, A.; Zugenmaier, P. J Appl Polym Sci 1997, 63, 9.
13. Swaminarayan, S.; Charbon, C. Polym Eng Sci 1998, 38, 4.
14. Charbon, C.; Swaminarayan, S. Polym Eng Sci 1998, 38, 4.
15. Yan, S.; Yang, D. J Appl Polym Sci 1997, 66.
16. Wang, C.; Hwang, L. M. J Polym Sci, Part B: Polym Phys 1996, 34.
17. Fillon, B.; Thierry, A.; Lotz, B.; Wittman, J. C. J Therm Anal 1994, 42.
18. Benderly, A.; Siegmann; Narkis, M. J Polym Eng 1997, 17, 6.
19. Prime, R.; Whelihan, E.; Burns, J. ANTEC 1988.
20. Hornsby, P. R.; Hinrichsen, E.; Tarverdi, K. J Mater Sci 1997, 32, 2.

21. Petrovic, Z. S.; Martinovic, B. ; Divjakovic, V.; Budinski-Simendic, J. J Appl Polym Sci 1993, 49.
22. Wolff, S.; Wang, M. J.; Tan, E. H. Rubber Chem Technol 1993, 66.
23. LeBlanc, J. L. J Appl Polym Sci 1997, 66.
24. Bigg, D. M. Polym Eng Sci 1982, 22.
25. Marquadrt, W. Haake Mess-Technik GmbH u. Co. 1994, V94/89E.
26. Poslinski, A. J.; Ryan, M. E.; Gupta, R. K.; Seshadri, S. G.; Frechette, F. J. Polym Eng Sci 1988, 28.
27. Lakdawala, K.; Salovey, R. Polym Eng Sci 1985, 25.
28. Altenberger, A. R.; Dahler, J. S. Int J Thermophys 1986, 7.
29. Ghofraniha, M.; Salovey, R. Polym Eng Sci 1988, 28.
30. Kaynak, A.; Polat, A.; Yilmazer, U. Mat Res Bull 1996, 31, 10.
31. Sengupta, P. K.; Mukhopadhyay, D. J Appl Polym Sci 1994, 51.
32. Alig, R. L. Technical Data Sheet from Applied Sciences, May 1996.
33. Anderson, D. P.; Ting, J. M.; Lake, M. L.; Alig, R. L. 22nd Biennial Conference on Carbon; American Chemical Society; San Diego, CA, 1995.
34. Alig, R. L.; Ting, J. The European Carbon Conference Carbon 96; Newcastle, UK, July 1996.
35. Tibbetts, G. G.; Devour, M. G.; Rodda, E. J. Carbon 1987, 25, 3.
36. Tang, B. Z.; Xu, H. Macromolecules 1999, 32.
37. Dagani, R. Chemical Engineering News, June 7, 1999.
38. www.apsci.com/asi (Applied Sciences).
39. www.fibrils.com (Hyperion Catalysis International).
40. MSDS Marlex, HLM-020 Polypropylene; Philips Sumika, July 1997.
41. Velasco, J. I.; De Saja, J. A.; Martinez, A. B. J Appl Polym Sci 1996, 61.
42. Tan, J. K.; Kitano, T.; Hatakeyama, T. J Mat Sci 1990, 25.
43. Bogoeva-Gaceva, G.; Janevski, A.; Grozdanov, A. J Appl Polym Sci 1998, 67.